

UDC 621.431.75

DOI: <https://doi.org/10.20535/0203-3771502025347474>Ortamevzi Gurkan¹ Ph.D.

EFFECTS OF GYROSCOPIC FORCES ON THE AIRCRAFT ENGINE MOUNT IN CASE OF ACROBATIC MOVEMENTS

Уа

У цій статті досліджується міцність моторами часто використовуваних надлегких гвинтових двигунів. Вихідні показники напруги та коефіцієнту запасу оцінені, зосереджуючись на зонах зварювання моторами, на яку впливають зусилля та сила тяги, які виникають особливо під час пілотажу. Розроблено мотораму для часто використовуваного двигуна, створено її 3D-модель і розрахункову сітку. Створена розрахункова сітка моторами змодельована при різних навантаженнях методом скінченних елементів.

En

In this article, the strength of the engine mounts of frequently used propeller ultralight engines was investigated. Especially, the stress and safety factor outputs of the mount, which affects the forces and thrust force generated during acrobatic movements, were evaluated by focusing on the welded areas. A mount was designed for a frequently used engine, a 3D model and a mathematical mesh model were created. The mathematical mesh model created was simulated at different loads using the finite element method.

Introduction

When designing engine mounts, thrust force is the most important force. Especially in flights where aerobatic movements, i.e. hard yaw, pitch and roll movements are intense; these forces can push the limits of the strength of the engine mounts. Even in an aircraft not designed for aerobatic movements, if hard pitch and yaw movements are made, the data in this article will shed light on the control of weak areas of the mount. When choosing a propeller, aircraft manufacturers and users should pay attention to the fact that the effect of the propeller weight will affect the strength of the mount as well as the engine.

Aircraft manufacturers should be very careful about the gyroscopic forces that can be very variable, especially the Coriolis force, which has a great effect on the strength of the engine mount [1, 2, 3, 4]. The mount is one of the most critical parts affected in an aircraft subjected to acrobatic movements. The mount is a part that directly affects flight safety. Especially in hard pitch and yaw movements, the welded areas of the mount are under intense stress. This situation can cause cracks that cannot be easily detected, or the integrity of the mount is damaged. In addition, the increase in the weight of the propeller increases this stress [5, 6, 7]. The Coriolis force, which is one of the gyroscopic forces, does not occur in the roll movement if the propeller shaft is on the

¹ Alanya Alaaddin Keykubat University

longitudinal axis or very close to it, or it occurs in a very small amount. Therefore, the forces created by the roll movement will not be simulated in this study. The rotation of the propeller shaft 90° around the lateral axis and the vertical axis by the yaw and pitch movements will create large Coriolis forces. The centrifugal force, which is one of the forces acting on an aircraft propeller without dynamic balance, is ignored for this study because the resultant force on the shaft will be zero [8, 9, 10].

Statement of the problem

This article aims to investigate the effects of a different weighted aircraft propeller change on the engine mount when the aircraft operator or manufacturer makes a change for an aircraft performing aerobatic movements and the distribution and magnitude of stress to which the engine mount is subjected during aerobatic movements. Although the weak areas of the engine mount against cracks or breaks when an aircraft not designed for aerobatic movements is subjected to hard pitch, yaw and roll movements.

3D Model and Mathematical Mesh Model

Let's consider an engine mount manufactured for a commonly used single-engine aircraft and analyze the strength of the welded areas (weak areas) of this mount.

In the study, a mount for an engine manufactured for a frequently used single-engine aircraft will be designed. The strength status of the welded areas or weak areas of this mount against the forces to which the mount is exposed will be analyzed. A 3D model and mathematical mesh model of this mount will be created. The force package consisting of the thrust force created by the engine and theoretically created gyroscopic forces, Coriolis force, and other inertial forces will be applied to the mount from the welded areas. The behaviors of the mount will be examined under these forces and the weak areas will be determined, and especially the areas joined by welding will be increased by using dense mesh for analysis details. The stress status of the mount and the safety factor indicator will be reported for these weak areas.

A 3D model and mathematical mesh model of this mount were created. The force package consisting of the thrust force created by the engine and theoretically created gyroscopic forces, Coriolis force, and other inertial forces were applied to the mount from the welded areas. The behaviors of the mount were examined under these forces and the weak areas were determined, and especially the areas joined by welding were increased by using dense mesh for analysis details. The stress status of the mount and the safety factor indicator were reported for these weak areas.

Inertial and gyroscopic forces acting on a propeller [11]: The change in the speed vectors advert to the accelerated motions of the rotating propeller mass that generate their inertial and gyroscopic forces f_{in} and the inertial torque T_{in} acting around axis oy that is expressed by the equation (1).

$$T_{in} = f_{in}x_m = ma_zx_m, \quad (1)$$

where T_{in} is the torque generated by the inertial force of propeller mass F_{in} ; a_z is the acceleration of the blade's mass m ; along axis oz ; and $x_m = r\cos\alpha$ is the distance to the mass location along axis ox .

Coriolis forces acting on a propeller [11]: Coriolis theory is used to determine the forces occurring during the roll, yaw and pitch movements of the aircraft. The absolute acceleration \vec{a} of a point undergoing compound motion is equal to the vector sum of; the relative acceleration \vec{a}_r , the translational (or transport) acceleration \vec{a}_e and the Coriolis acceleration \vec{a}_c :

$$\vec{a} = \vec{a}_e + \vec{a}_r + \vec{a}_c. \quad (2)$$

The last term in the acceleration addition theorem is called the Coriolis acceleration:

$$\vec{a}_c = 2\vec{\omega}_e \times \vec{v}_r, \quad (3)$$

where: \vec{a}_c : Coriolis acceleration (vector form), $\vec{\omega}_e$: Angular velocity of the moving reference frame, \vec{v}_r : Relative velocity of the particle in the moving frame and \times : Vector (cross) product.

The magnitude of the Coriolis acceleration is given by:

$$a_c = 2\omega_e v_r \sin(\theta), \quad (4)$$

where: ω_e : Magnitude of angular velocity, v_r : Magnitude of relative velocity, θ : Angle between vectors ω_e and v_r .

The resistance torque generated by the Coriolis force of the blade's mass is expressed by the equation (2).

$$T_{cr} = -f_{cr}y_m = -ma_zy_m, \quad (5)$$

where T_{cr} is the torque generated by Coriolis force f_{cr} of the rotating blade's mass m ; a_z is the acceleration of the mass along axis oz ; and $y_m = r\sin\alpha$, is the distance to the mass location along axis oy ; the sign (-) means the action in the clockwise direction.

As seen in Fig. 1, *a*, since θ angle is equal to 0 for the roll motion of the aircraft,

$$\sin(\theta) = 0 \Rightarrow 0 a_c = 0 \text{ and } f_{cr} = 0.$$

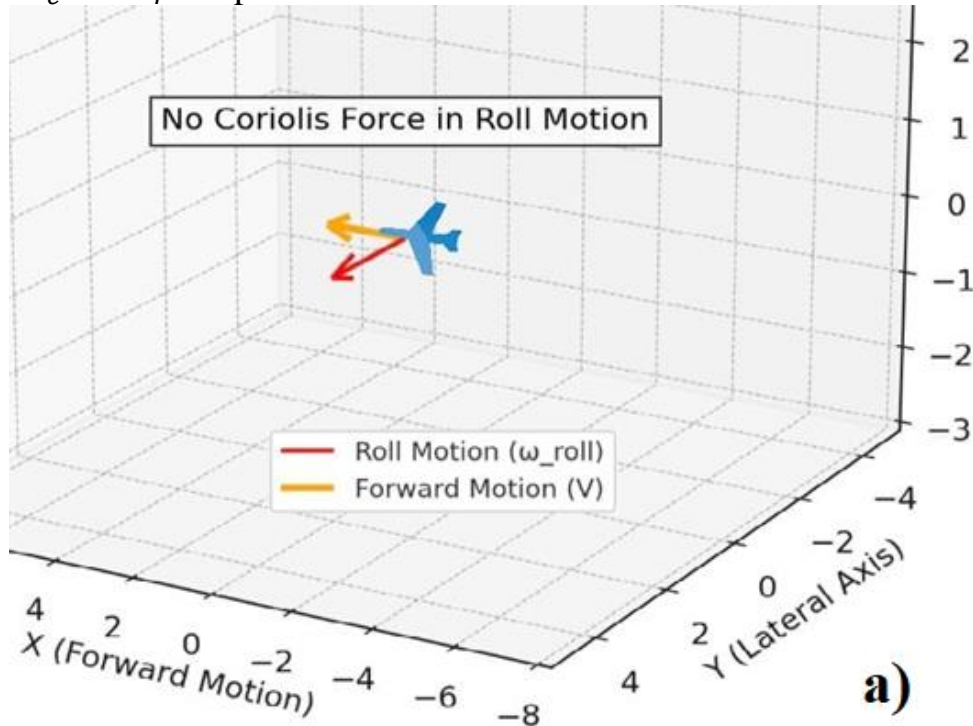
According to the 4-th formula for the pitch movement of the aircraft in Fig. 1. *b*,

$$\sin(\theta) = 1 \Rightarrow a_c = 2\vec{\omega}_e \times \vec{v}_r \text{ and } f_{cr} = ma_c.$$

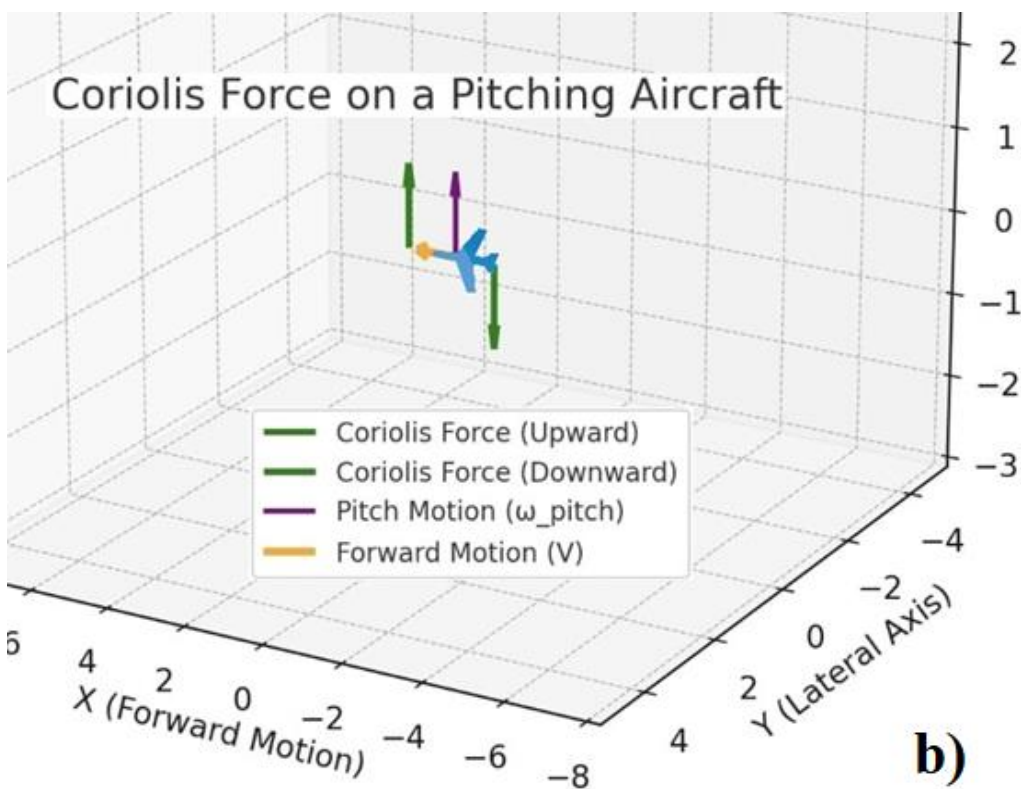
According to the 4-th formula for the yaw movement of the aircraft in Fig. 1. c,

$$\sin(\theta) = 1 \Rightarrow a_c = 2\bar{\omega}_e \times \vec{v}_r \text{ and } f_{cr} = ma_c.$$

The Coriolis force does not occur in roll motion in an aircraft because vectors ω_e and v_r are parallels.



a)



b)

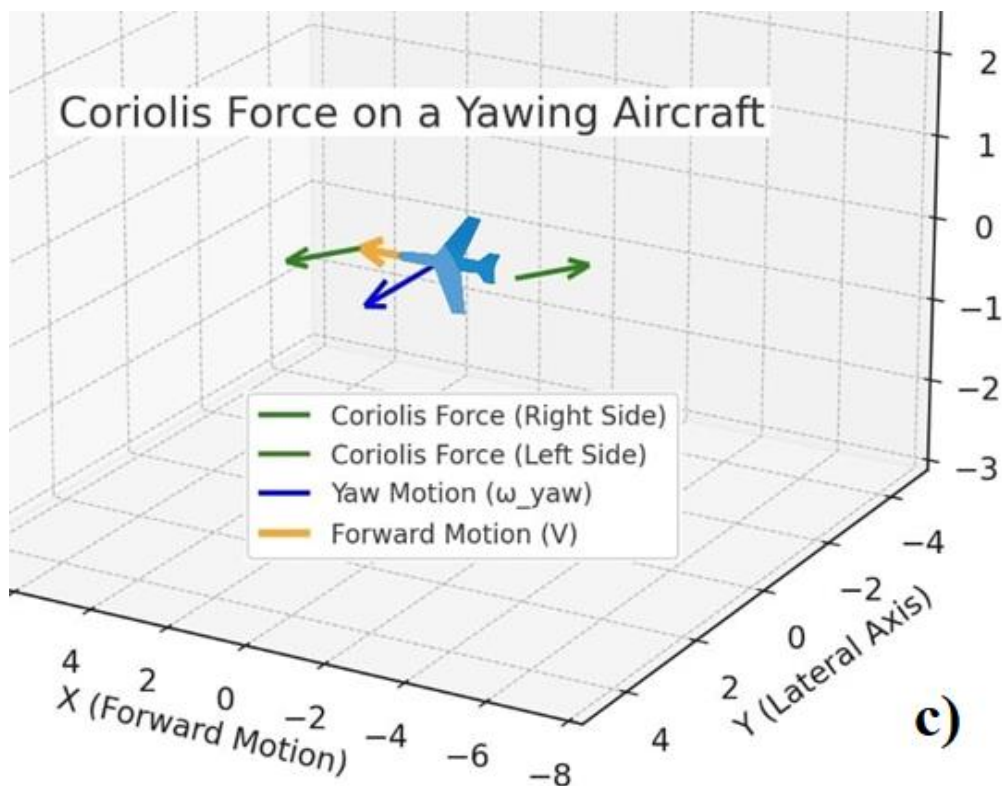


Fig. 1. The Coriolis forces; a)for roll, b)for pitch and c)for yaw movements

The force package that will act on the mount can be calculated using formulas (1), (2). According to formulas (1), (2), the biggest factor that increases the size of the force package will be the acceleration of the mass. The acceleration of acrobatic movements is very variable. However, propeller dynamic balance tolerances and/or propeller assembly error tolerances will also increase this force. Therefore, it was deemed logical to simulate these force packages in a high range of 0-2000 N.

An example of an aircraft engine's connection areas and mount, $L1-L6$ are the connecting bolt holes and P is the axis of the propeller commonly used on single-engine aircraft, is shown in Fig. 2.

The 3D model and mathematical mesh model of the mount were created to determine the stress state and safety factor to be simulated under specified forces. Since the weld regions were predicted as weak regions, they were meshed more densely. The weld regions were numbered so that the regions could be evaluated separately. The 3D model and mathematical mesh model of the mount are shown in Fig. 3. and Fig. 4. The statistics of mesh for the mathematical mesh model consists of 777495 nodes and 438763 elements.

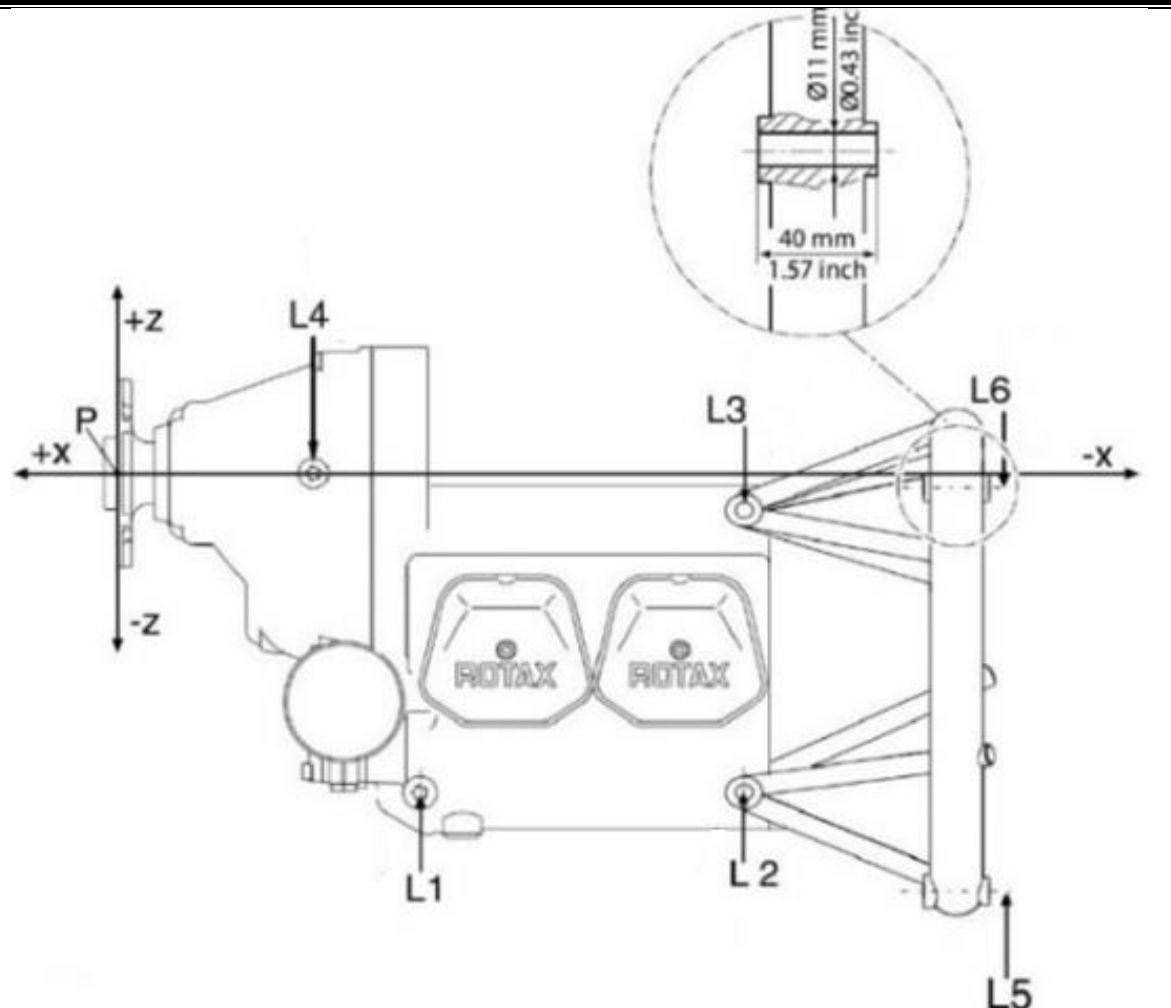


Fig. 2. Attachment points of engine and an example of a mount

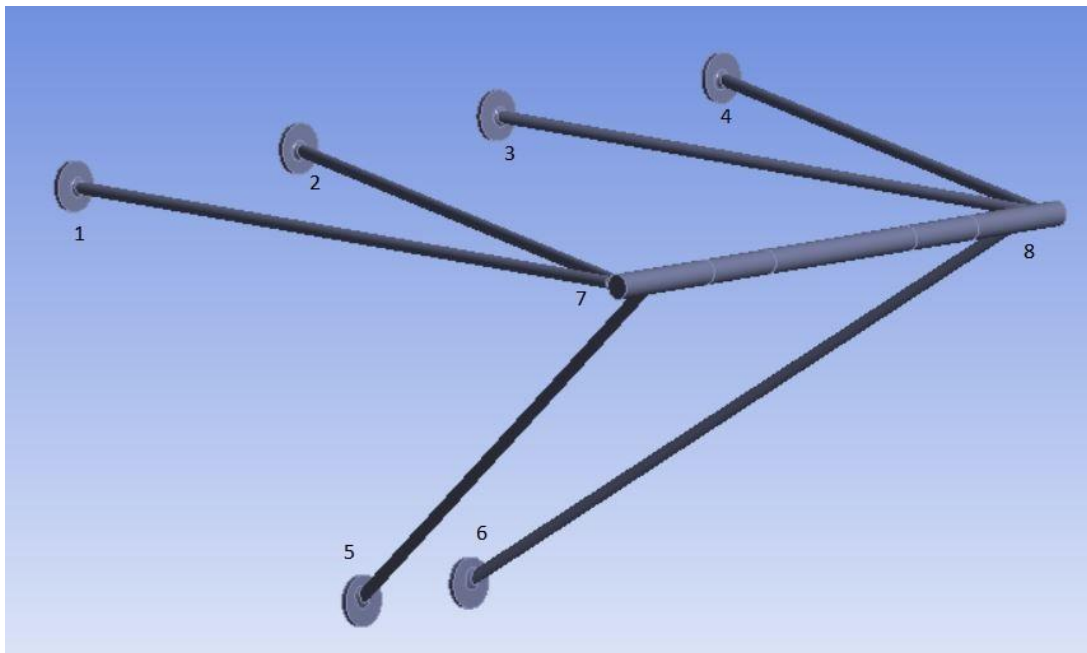


Fig. 3. 3D Model of mount (junction areas are defined with numbers)

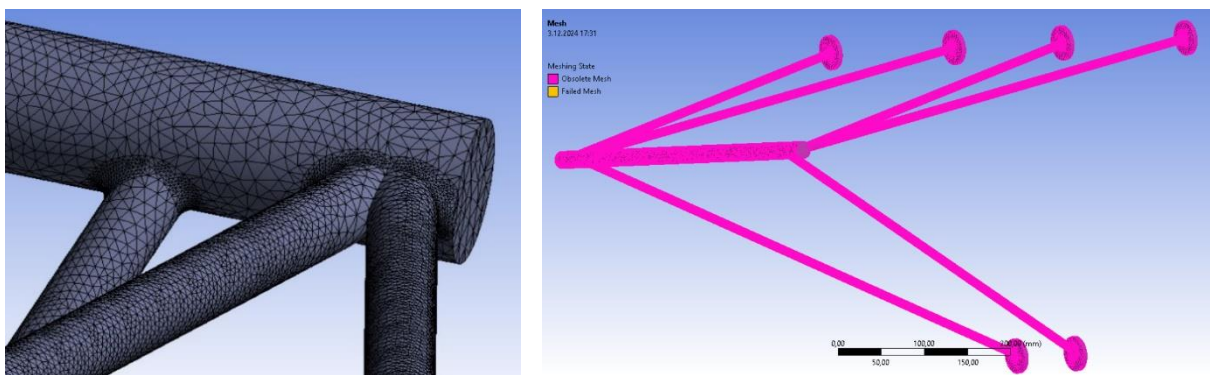


Fig. 4. Mathematical mesh model of mount

The thrust force increased by 400 N between 0-2000 N as 2000 and 1000 N, and the Coriolis forces generated during pitch and yaw movements were applied to the mount only to the left for yaw movement and as remote force for both up and down for pitch movement. Combinations of these forces were made and 36 different situations were simulated [11]. The resultant force for the largest force combination in the pitch up movement is shown in Fig. 5.

The stress conditions and safety factor values of the mount were analyzed using the finite element method. The stress and safety factor values of the force combination, where the thrust force is 2000 N and the Coriolis forces created by the yaw left, pitch up, pitch down movements are increased by 400 N in the range of 0-2000 N, are graphed in Fig. 7 according to the numbered welding areas indicated in Fig. 3. The stress intensity of the mount is shown in Fig. 6.

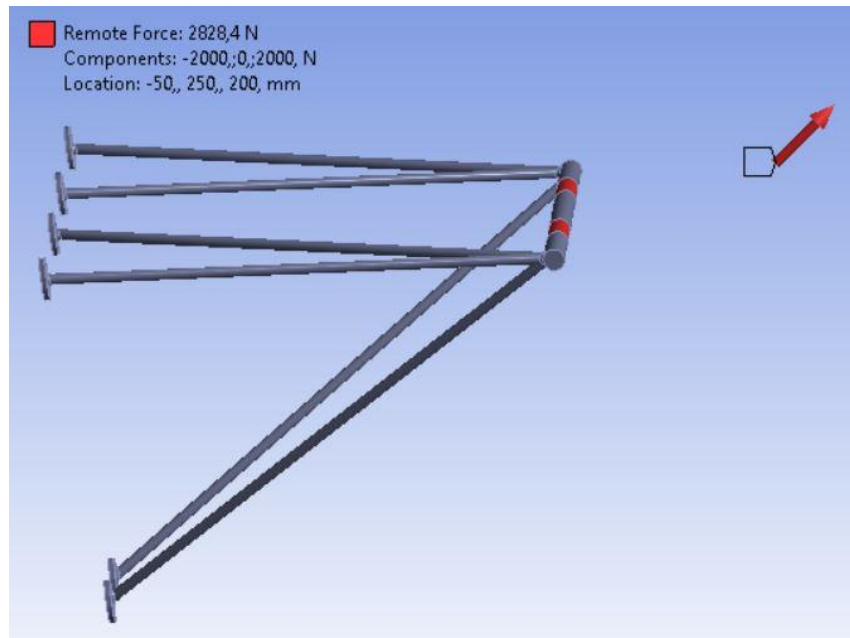


Fig. 5. Simulation of forces applied on the mount

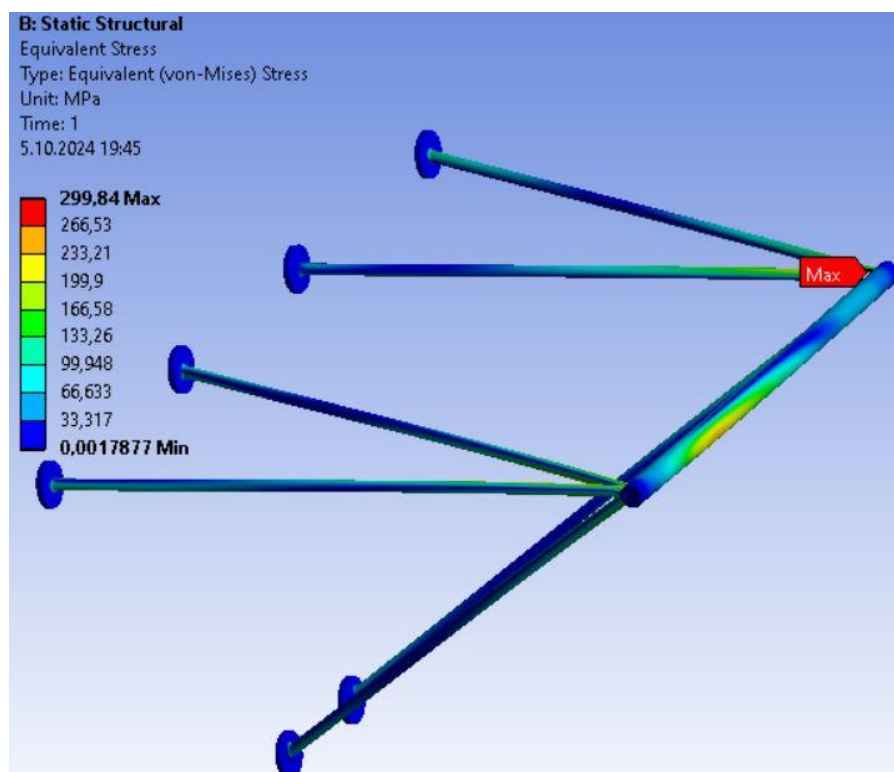


Fig. 6. Stress intensity

While we can show the stress distribution only with visual colors, we can also graph the average stress magnitude and average safety factor values obtained from the analysis to make them more understandable in weak areas. Graphs have been obtained for each different scenario. These situations may occur instantaneously or for a period of time. In a scenario of a situation that is constantly repeated, for example, propeller blades that are not mounted at equal

angles, this static analysis may not be sufficient. In such cases, more reliable results can be obtained if transient analysis is performed.

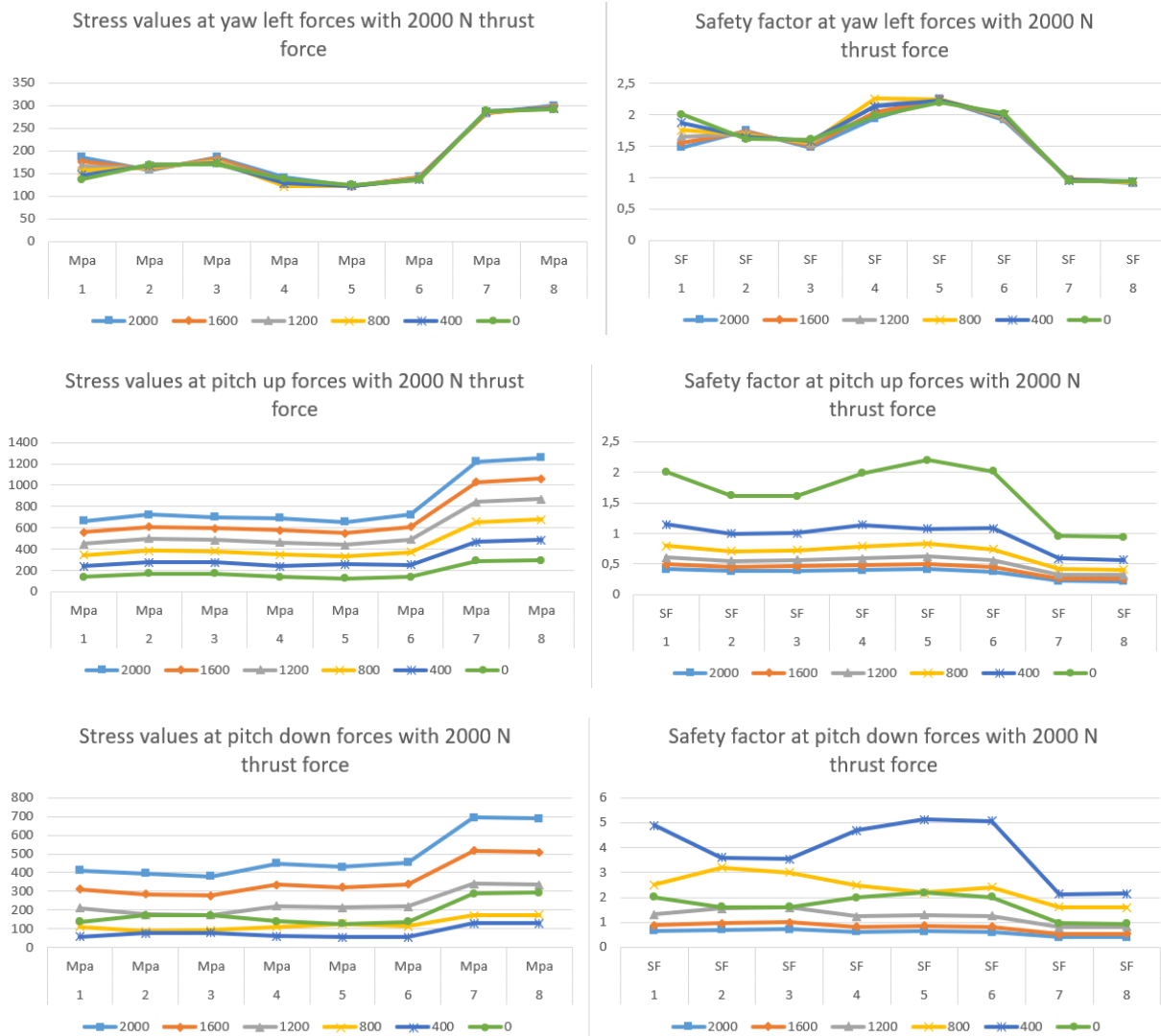


Fig. 7. Stress and safety factor values according to the numbered welding areas specified in Fig. 1

The stress and safety factor values of the force combination, where the thrust force is 1000 N and the Coriolis forces created by the yaw left, pitch up, pitch down movements are increased by 400 N in the range of 0-2000 N, are graphed in Fig. 8 according to the numbered welded areas indicated in Fig. 3.

According to the analyses, Figures 5-8 show that the maximum equivalent stress occurs in the 7th and 8th weld zones, with a noticeable magnitude. At an engine thrust force of 2000 N and a Coriolis force of 400 N, the stress in these zones reaches approximately 1200 MPa, and the factor of safety falls below 1. Specifically, the equivalent stress in pitch-up motion is twice as high as in pitch-down motion and four times as high as in yaw motion.

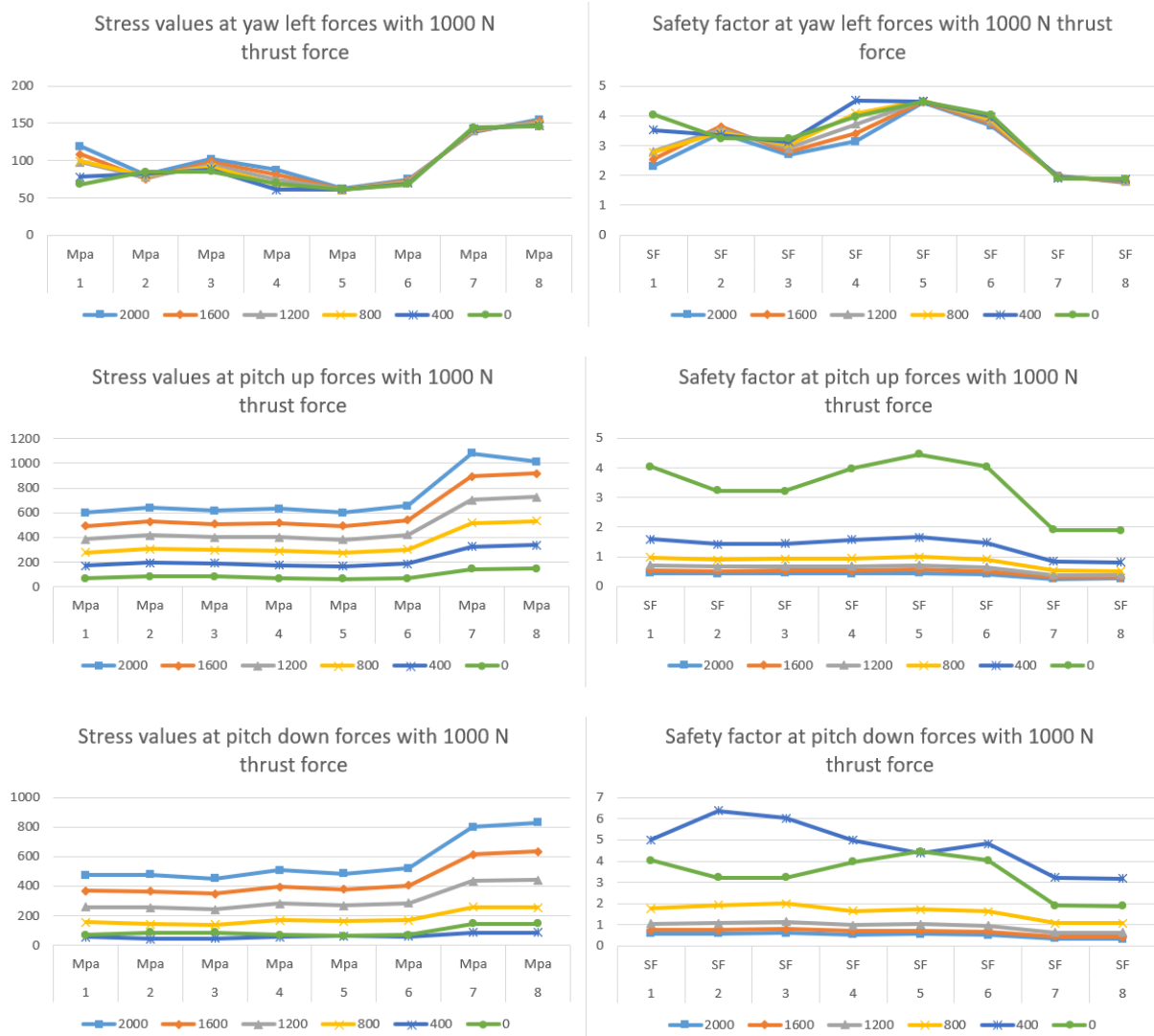


Fig. 8. Stress and safety factor values according to the numbered welding areas specified in Fig. 3

The equivalent stress in weld zones 1-6 is approximately 45% less in pitch and yaw motions than in weld zones 7-8. Theoretically, analyses have shown that under critical loading conditions, concentrated stresses can occur in the 7th and 8th weld zones of the engine mount.

This analysis quantitatively examines the effects of propeller weight and the magnitude of the forces generated during aerobatic maneuvers on engine mounting safety. The resulting stress and safety factor distribution data provide insights for aircraft manufacturers and users in assessing engine mounting safety in the event of propeller replacement or performance upgrades.

Conclusion

Studies have shown that the weight of the propeller, chosen by aircraft manufacturers or users, directly affects the strength of the joint of the engine mount in an aircraft subjected to acrobatic movements.

The magnitude of the Coriolis force creates higher stresses and lower safety coefficient values, especially in the 7th and 8th welded attachment zones, as well as during pitch up and down movements, than in yaw motion. Therefore, all welding areas of the attachment, especially in the 7th and 8th (weak areas) zones, should be carefully checked for cracks.

During flight, where Coriolis forces exceeding 400 N are generated, the engine mount developed in this article should not be used. It can be predicted that the joint areas of the design should be produced with stronger materials that is the yield strength is higher than 500 MPa and/or larger radius geometries.

According to the results of analyses conducted using the Finite Element Method, under a thrust force of 2000 N and Coriolis forces of up to 400 N, the 7th and 8th weld zones experience a stress of 320 MPa and a safety factor of less than 1.2 at maximum yaw; a stress of 1200 MPa and a safety factor well below 1 during pitch-up; and a stress of 700 MPa and a safety factor close to 1 during pitch-down. These zones are at critical risk of fracture during acrobatics. The most dangerous acrobatic movement in these zones has been observed to be pitch-up.

References

1. *P. Magryta and K. Pietrykowski*, “Simulation research of the strength of an engine mount in an aircraft piston diesel engine,” in *Journal of Physics: Conference Series*, 2021, vol. 2130, no. 1, p. 12017.
2. *T. Shim and D. Margolis*, “Controlled equilibrium mounts for aircraft engine isolation,” *Control Eng. Pract.*, vol. 14, no. 7, pp. 721–733, 2006.
3. *S. Ramesh, R. Handal, M. J. Jensen, and R. Rusovici*, “Topology optimization and finite element analysis of a jet dragster engine mount,” *Cogent Eng.*, vol. 7, no. 1, p. 1723821, 2020.
4. *L. Jørgensen Honarchian Saki*, “Design of Aero Engine Mount Structure.” 2023.
5. *R. Usubamatov*, “A rotating body about the fixed point is subjected by inertial torques,” *Int Robot Autom. J*, vol. 7, no. 3, pp. 75–76, 2021.
6. *R. Usubamatov and T. Zhumaev*, “Inertial Forces Acting on a Propeller of Aircraft,” *Open Aerosp. Eng. J.*, vol. 7, no. 1, 2018.
7. *Г. Ортамееви*, “The effect of gyroscopic force on the life of the uav’s propeller shaft bearing under intense acrobatic movements,” *Механіка гіроскопічних систем*, no. 46, pp. 120–130, 2023.
8. *J. Morris*, “Some Dynamical Characteristics of Propellers,” *Aeronaut. J.*, vol. 38, no. 288, pp. 987–997, 1934.
9. *A. Otter, J. Murphy, and C. J. Desmond*, “Emulating aerodynamic forces and moments for hybrid testing of floating wind turbine models,” in *Journal of Physics: Conference Series*, 2020, vol. 1618, no. 3, p. 32022.

10. *P. C. Teixeira and C. E. S. Cesnik*, “Propeller effects on the response of high-altitude long-endurance aircraft,” *AIAA J.*, vol. 57, no. 10, pp. 4328–4342, 2019.
11. *I. Ivanov, V. Myasnikov, and B. Blinnik*, “Study of dynamic loads dependence on aircraft engine mount variant after fan blade-out event,” *Vibroengineering Procedia*, vol. 26, pp. 1–6, 2019.